Free vibration of functionally graded SWNT reinforced aluminum alloy beam

Abdellatif Selmi[1], Awni Bisharat[2]
[1]Prince Sattam Bin Abdulaziz University, College of Engineering, Civil Engineering Department,
B.P. 655, Al-Kharj 11942, Saudi Arabia
[2]Prince Sattam Bin Abdulaziz University, College of Engineering, Mechanical Engineering Department,
B.P. 655, Al-Kharj 11942, Saudi Arabia
[1]Ecole Nationale d'Ingénieurs de Tunis (ENIT), Civil Engineering Laboratory,
B.P. 37, Le belvédère 1002, Tunis, Tunisia
[1]Corresponding author
E-mail: [1]*selmi_fr2016@yahoo.com*, [2]*bisharatawni@yahoo.com*

Abstract. Aluminum alloy (Al-alloy) reinforced with Single walled carbon nanotubes (SWNT), which represents an important industrial application, is studied. Different beam theories (BT) are applied to investigate functionally graded (FG) beams made of Al-alloy reinforced with randomly oriented, straight and long SWNT. The Rayleigh-Ritz method is used to estimate the beam frequencies. First, the Mori-Tanak (M-T) homogenization technique is used to predict the effective material properties of the beams. Second, results from BT are verified against finite element (FE) simulations. Next, a parametric study is carried out in order to investigate the influence of SWNT volume fractions, SWNT distributions and beam edge-to-thickness ratios on the vibration behavior of the FG beam. Results demonstrate the important effect of the studied parameters on the dynamic behavior of the FG SWNT reinforced Al-alloy composite beams.

Keywords: aluminum alloy, SWNT, functionally graded beam, free vibration.

1. Introduction

SWNT are an important variety of carbon nanotubes. SWNT possesses exceptional mechanical, electrical and thermal properties. The application of the concept of FGM to SWNT composites has led to design different components satisfying particular properties [1]. FG SWNT reinforced composites are a new composite material having different applications in aerospace, defense, energy, automobile, medicine, structural and chemical industry [2]. The efficiency of SWNT as reinforcement can be attributed to the load transfer mechanism from matrix to SWNT at nanoscale. Interfacial bonding in the interphase region between embedded SWNT and its surrounding polymer is a key factor for the load transfer and reinforcement phenomena [3].

Al-alloys are broadly used in diverse applications like aerospace, automotive as well as chemical industries due to its distinct properties as compared to other metals [4]. Because of the extraordinary physical and chemical properties of SWNT, reinforcement of Al-alloys with this type of material leads to huge changes in its properties like greater strength, improved stiffness, reduced density, improved high temperature properties, improved abrasion and wear resistance [5, 6].

Most of the studies in SWNT reinforced composites are concentrated on the effect of the reinforcement volume fraction on the mechanical properties [7, 8] but research on vibration analysis of FG SWNT reinforced composite structures is limited to a few published articles. In the following, some of the recent published works on the dynamic characteristics of FG SWNT reinforced composite beams.

Heshmati and Yas [9] investigated the improvement of the fundamental natural frequency of FG SWNT reinforced polymer composite beam. The governing equations are found using the Euler-Bernoulli beam theory. The effect of SWNT agglomeration, distribution and boundary

conditions on the dynamic behavior of the beam is found to be very important. The work carried out recently by Shenas et al. [10] presented the free vibration behavior of the pre-twisted FG SWNT reinforced composite beams in thermal environment. The third-order shear deformation beam theory is used to obtain the governing equations. The Chebyshev-Ritz method is used to determine the free vibration eigenvalue equations. The FG beam is found to be sensitive to the pre-twist angle and to the temperature. The free vibration of nanocomposite Timoshenko FG beams reinforced with SWNT resting on an elastic foundation is studied by Yas and Samadi [11]. The SWNT are assumed to be aligned and straight with a uniform layout. The rule of mixture is used to describe the effective material properties of the nanocomposite beams. The governing equations are derived through Hamilton's principle and then solved by using the generalized differential quadrature method. Effects of SWNT volume fraction, foundation stiffness parameters, slenderness ratios, SWNT distribution and boundary conditions on natural frequency are estimated. Ke et al. [12] investigated the nonlinear vibration of aligned straight SWNT FG beams based on Timoshenko beam theory and von Karman geometric nonlinearity. The effect of the vibration amplitude, volume fraction of SWNT, ratio of length to thickness, boundary conditions and SWNT distribution were taken into account to characterize the nonlinear vibration of the beams. In light of von Karman geometric nonlinearity assumptions and the first-order shear deformation beam theory, Wu et al. [13] studied the nonlinear vibration of FG SWNT reinforced composite beams with initial imperfection. The Ritz method is applied to derive the nonlinear eigen frequency. Ansari et al. [14] dealt with the nonlinear vibration behavior of nanocomposite beams reinforced with SWNT based on the Timoshenko beam theory along with von Karman geometric nonlinearity. Poly methyl methacrylate (PMMA) is considered as the matrix. The vibration of cantilever FG SWNT beam subjected to compressive axial force is studied by Nejati et al. [15]. The two-dimensional elasticity theory and Hamilton's principle are used to determine the stability and motion equations. These equations are discretized using the generalized differential quadrature method. The influence of graded agglomerated SWNT, and the effect of axial forces exerted on the natural frequencies of FG beam are investigated. Yas and Heshmati [16] worked on dynamics of FG nanocomposite beams reinforced with randomly oriented SWNT. The dynamic characteristics of the FG beam are predicted using Timoshenko and Euler-Bernoulli beam theories. It is found that under the action of moving load, FG SWNT beam with symmetrical distribution gives superior properties than that of unsymmetrical distribution.

To the author's knowledge, the free vibration of FG SWNT reinforced Al-alloy composite beams, which represent an important industrial application, has not been investigated.

In a variety of dynamic problems, exact solutions may not be obtained, and one has to employ approximate methods. The Rayleigh-Ritz method is an approximate numerical method used extensively in several research sectors, but especially in the analysis of structural members [17]. The method can be used for both continuous and discrete systems. It is based on a linear expansion of the solution in terms of admissible functions [18]. In vibration problems, the frequencies are deduced from a quotient with potential energy being the numerator and kinetic energy function being the denominator. This quotient is called the Rayleigh quotient. The expansion coefficients are obtained using the principle of minimum potential energy [18].

Based on the classical beam theory (CBT), the Timoshenko beam theory (TBT) and the parabolic shear deformation beam theory (PSDBT), the present research focuses on the free vibration of FG SWNT reinforced Al-alloy composite beams. The Rayleigh-Ritz method is used to determine the frequencies.

The objective is to study the effects of SWNT volume fraction, SWNT distribution pattern, beam slenderness ratio and the BT on the natural frequencies of FG SWNT reinforced Al-alloy composite beams. To validate the present analysis, comparative studies are carried out with available results from the existing literature and with performed FE simulations.

The paper has the following outline. In Section 2, the homogenized properties of SWNT reinforced Al-alloy composite are determined using the two level (M-T, M-T) scheme. Section 3 details the mathematical modeling on vibration of randomly oriented FG SWNT reinforced

Al-alloy composite beams based on the BT and the Rayleigh-Ritz method. Section 4 presents the numerical results of free vibration of FG SWNT reinforced Al-alloy composite beams using the mentioned BT and FE simulations. The validation of obtained results and parametric study are discussed in the same Section 4. Lastly, Section 5 summarizes the results and conclusions.

2. Material properties of FG SWNT reinforced Al-alloy composite beams

2.1. Mechanical properties of Al-alloy, SWNT and SWNT/Al-alloy composites

The Young's modulus, the Poisson's ratio and the density of Al-alloy taken in this paper are respectively; $E = 70$ GPa, $v = 0.33$ and $\rho = 2700$ Kg/m^3 [19] while the Young's modulus and the Poisson's ratio of the homogenized graphene sheet that constitute the SWNT are determined by the author using a homogenization method based on the energy equivalence and have been found to be 2520 GPa and 0.25, respectively [7]. The density of the armchair SWNT with chiral index of (10, 10) is 1330 Kg/m^3 [20].

A mean field homogenization scheme named two-level (M-T/M-T) is selected to predict the mechanical properties of SWNT/Al-alloy composites.

The two-level procedure was proposed by Friebel et al. [21] for coated inclusion-reinforced materials. The methodology is illustrated on Fig. 1. Each SWNT is seen (deep level) as a two-phase composite (graphene sheet with cavities) which, once homogenized, plays the role of a homogeneous reinforcement for the matrix material (high level). In the first level of the two-level procedure, the graphene matrix containing many small ellipsoidal cavities (having the same shapes and aspect ratios as the actual ones) is homogenized. The homogenization of the matrix material reinforced with homogeneous reinforcement is performed in the second level. In this paper, choosing Mori-Tanaka (M-T) for both levels, the scheme is labeled "two-level (M-T/M-T)".
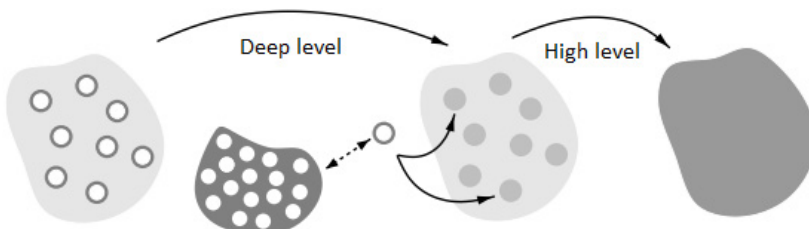
Fig. 1. Schematic view of the two-level homogenization procedure for the effective properties of SWNT composites. For each level a two-phase homogenization model is required

The rule of mixture is adopted to determine the density of the mentioned composite. The variations of Young's modulus, Poisson's ratio and density, as a function of reinforcement volume fraction, V, of 3D randomly oriented and long SWNT/Al-alloy composites are reported in Table 1.

Interpretation: From Table 1, it is deduced that the reinforcing effect of SWNT is very important and as the SWNT volume fraction in the Al-alloy increases, the Young's modulus increases rapidly. For an Al-alloy comprising 10 % of SWNT, the Young's modulus, E, is increased by a factor of 1.4 but the Poisson's ratio and the density decreases by a factor of 1.06 and 1.05, respectively.

Table 1. SWNT/Al-alloy composite with 3D randomly oriented and long reinforcements

V (%)	E (GPa)	N	ρ (Kg/m^3)
0	70	0.33	2700
1	72.88	0.327	2686.3
3	78.60	0.323	2658.9
5	84.28	0.319	2631.5
10	98.33	0.311	2563

2.2. Properties of FG materials

A straight simply supported FG beam of length L, width b, and thickness h is shown in Fig. 2.
In the present study, the volume fraction of SWNT is assumed to be graded in the thickness direction so that the material properties of the beam vary continuously according to power-law form as shown in Figs. 3, 4.
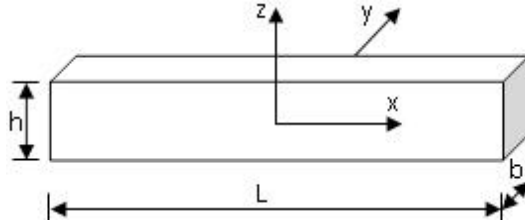

Fig. 2. Beam element with Cartesian coordinates
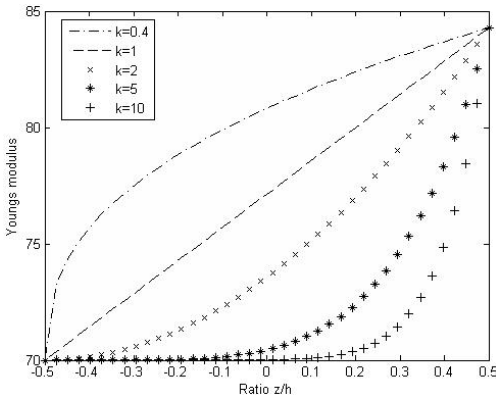
Fig. 3. Variation of Young's modulus through the thickness direction of the beam
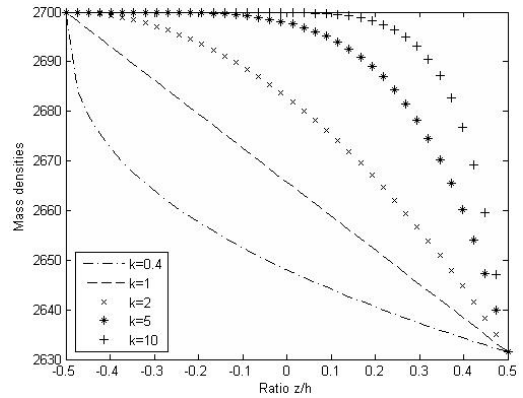
Fig. 4. Variation of mass density through the thickness direction of the beam

The considered power-law variation is:

$$P(z) = (P_c - P_a)\left(\frac{z}{h} + \frac{1}{2}\right)^k + P_a. \tag{1}$$

P_a and P_c stand for the values of the material properties of Al-alloy and SWNT/Al-alloy composite, respectively. Therefore, the bottom surface of the beam is Al-alloy, whereas its top surface is SWNT reinforced Al-alloy composite. Hereafter, for the top surface, 5 % and 10 % SWNT volume fractions are considered.

3. Numerical modeling and formulation

Let's assume the deformation of FG beam in the x-z plane and designate the displacement components in the x and z directions by u_x and u_z, respectively. Based on the BT, the axial and transverse displacement of any point of the beam are respectively:

$$u_x(x, z, t) = u(x, t) - zw_{,x}(x, t) + \phi(z)v(x, t),$$
$$u_z(x, t) = w(x, t), \tag{2}$$

where u and w denote the axial and the transverse displacement of any point on the neutral axis respectively, while v represents the effect of transverse shear strain on the neutral axis. $\phi(z)$

stands for the shape function and (x) indicates the partial derivative in terms of x. The present study is concerned with classical beam theory, CBT, Timoshenko beam theory, TBT, and parabolic shear deformation beam theory, PSDBT [22]. $\phi(z)$ for these BT are given as below [23]:

CBT: $\phi(z) = 0,$
TBT: $\phi(z) = z,$
PSDBT: $\phi(z) = z\left(1 - \dfrac{4z^2}{3h^2}\right).$

The strain energy, S, and the kinetic energy, T, of the beam at any moment are given as:

$$S = \frac{1}{2} \int_{-L/2}^{L/2} \int_A (\sigma_{xx}\varepsilon_{xx} + \tau_{xz}\gamma_{xz})dAdx, \tag{3}$$

$$T = \frac{1}{2} \int_{-L/2}^{L/2} \int_A \rho(z)\left[\left(\frac{\partial u_x}{\partial t}\right)^2 + \left(\frac{\partial u_z}{\partial t}\right)^2\right]dAdx, \tag{4}$$

where A and ρ are the area of cross-section and the mass density of the beam, respectively. σ_{xx}, τ_{xz}, ε_{xx} and γ_{xz} denote the normal stress, the shear stress, the normal strain and the shear strain, respectively

Assuming the harmonic displacement components:

$$\begin{cases} u(x,t) = U(x)\sin\omega t, \\ v(x,t) = V(x)\sin\omega t, \\ w(x,t) = W(x)\sin\omega t, \end{cases} \tag{5}$$

where $U(x)$, $V(x)$ and $W(x)$ are the respective amplitudes of the displacement components and ω is the natural frequency.

The substitution of the expressions of displacement components into Eqs. (3), (4) yields the maximum strain energy, S_{max}, and the maximum kinetic energy, T_{max} as:

$$\begin{aligned} S_{max} = \frac{1}{2} \int_{-L/2}^{L/2} &\left[A_{xx}\left(\frac{dU}{dx}\right)^2 - 2B_{xx}\left(\frac{dU}{dx}\right)\left(\frac{d^2W}{dx^2}\right) + D_{xx}\left(\frac{d^2W}{dx^2}\right) + 2E_{xx}\left(\frac{dU}{dx}\right)\left(\frac{dV}{dx}\right)\right. \\ &\left. -2F_{xx}\left(\frac{dV}{dx}\right)\left(\frac{d^2W}{dx^2}\right) + H_{xx}\left(\frac{dV}{dx}\right)^2 + A_{xz}V^2\right]dx, \end{aligned} \tag{6}$$

$$\begin{aligned} T_{max} = \frac{\omega^2}{2} \int_{-L/2}^{L/2} &\left[I_A(U^2 + W^2) - 2I_B U\left(\frac{dW}{dx}\right) + I_D\left(\frac{dW}{dt}\right)^2 + 2I_E UV\right. \\ &\left. +2I_F V\left(\frac{dW}{dx}\right) + I_H V^2\right]dx, \end{aligned} \tag{7}$$

where:

$$(A_{xx}, B_{xx}, D_{xx}) = \int_A Q_{11}(1, z, z^2)dA, \quad (E_{xx}, F_{xx}) = \int_A \Phi(z)Q_{11}(1, z)dA,$$

$$H_{xx} = \int_A [\Phi(z)]^2 Q_{11}dA, \quad A_{zx} = \int_A [\Phi'(z)]^2 Q_{55}dA, \tag{8}$$

and:

$$(I_A, I_B, I_D) = \int_A \rho(z)(1, z, z^2)dA, \quad (I_E, I_F) = \int_A \Phi(z)\rho(z)(1, z)dA,$$

$$I_H = \int_A [\Phi(z)]^2 \rho(z)dA. \tag{9}$$

The transformed stiffness constants are:

$$Q_{11} = \frac{E(z)}{1 - v^2}, \quad Q_{55} = \frac{E(z)}{2(1 - v)}.$$

Using the Rayleigh-Ritz method, the amplitudes of vibration can be expanded in terms of polynomial functions by the following series as:

$$U = \sum_{i=1}^n c_i \varphi_i, \quad V = \sum_{j=1}^n d_j \psi_j, \quad W = \sum_{k=1}^n e_k \chi_k,$$

where c_i, d_j and e_k are constants to be determined and φ_i, ψ_j and χ_k are known functions that must satisfy the boundary conditions of the problem. These admissible functions can be written as:

$$\varphi_i = fx^{i-1}, \quad i = 1,2,\dots,n,$$
$$\psi_j = fx^{j-1}, \quad j = 1,2,\dots,n,$$
$$\chi_k = fx^{k-1}, \quad k = 1,2,\dots,n.$$

For simply supported beams: $f = x^2 - (L/2)^2$ [24].

Consequently, by equating S_{max} and T_{max}, the Rayleigh Quotient ω^2 can be deduced. The principle of minimum potential energy implies that the partial derivatives of the Rayleigh Quotient with respect to each of the constants c_i, d_j, and e_k are nul. Accordingly, one can write:

$$\frac{\partial \omega^2}{\partial c_i} = 0, \quad i = 1,2,\dots,n,$$

$$\frac{\partial \omega^2}{\partial d_j} = 0, \quad j = 1,2,\dots,n, \tag{10}$$

$$\frac{\partial \omega^2}{\partial e_k} = 0, \quad k = 1,2,\dots,n.$$

Eq. (10) represents a set of $3n$ algebric equations in $3n$ unknowns c_1, c_n, d_1, d_n, and e_1, e_n. Its resolution requires considerable computation duration. Eq. (10) is then written in matricial form as:

$$([K] - \lambda^2[M])[\Delta] = 0, \tag{11}$$

where $[K]$ and $[M]$ are the dynamic stiffness and inertia matrices, respectively and $[\Delta]$ is the vector of unknown coefficients. The frequency parameters for free vibration problem are given by λ. Frequency parameters determined from this eigenvalue problem are investigated in the next section with the mentioned BT. Validation with the existing literature and with FE results are also reported.

4. Numerical results

In this section, the first three frequency parameters for the free vibration of simply supported FG beam are investigated using the above-mentioned beam theories. The effect of the distribution fashion of the SWNT volume fraction throughout the beam thickness, the effect of SWNT content in the beam top surface and the beam slenderness ratio are analyzed. The frequency parameter is expressed as:

$$\lambda = \frac{\omega L^2}{h}\sqrt{\frac{\rho_a}{E_a}}. \tag{12}$$

4.1. Convergence and validation of the analysis

4.1.1. Convergence analysis

In Tables 2-4, the convergence behavior of first three frequency parameters of simply supported FG beam with $L/h = 5$ and 5 % SWNT volume fraction on the beam top surface are reported. The increase in the number n of polynomial items in the admissible functions is checked using CBT, TBT and PSDBT.

Table 2. Convergence of first three frequency parameters of simply supported FG SWNT/Al-alloy beams using CBT for ($L/h = 5$) and 5 % SWNT content on the beam top surface

CBT	Al-alloy			$k = 5$		
N	λ_1	λ_2	λ_3	λ_1	λ_2	λ_3
2	3.2956	14.3779	16.7497	3.4988	14.7756	17.1114
3	2.9706	14.3779	16.6402	3.0621	14.774	17.0014
4	2.9706	11.3964	16.6401	3.0621	11.7342	16.9624
5	2.9697	11.3964	16.6401	3.0612	11.7342	16.9623
6	2.9697	11.3491	16.6401	3.0612	11.6859	16.9618
7	2.9697	11.3491	16.6401	3.0612	11.6859	16.9618
8	2.9697	11.3491	16.6401	3.0612	11.6857	16.9618
9	2.9697	11.3491	16.6401	3.0612	11.6857	16.9618
10	2.9697	11.3491	16.6401	3.0612	11.6857	16.9618

Table 3. Convergence of first three frequency parameters of simply supported FG SWNT/Al-alloy beams using TBT for ($L/h = 5$) and 5 % SWNT content on the beam top surface

TBT	Al-alloy			$k = 5$		
n	λ_1	λ_2	λ_3	λ_1	λ_2	λ_3
2	3.2955	13.5286	16.7497	3.3975	14.0428	17.0927
3	2.8384	13.4888	16.6402	2.9449	14.0038	16.9816
4	2.8300	9.5017	16.6402	2.9364	10.0211	16.9529
5	2.8225	9.4253	16.5059	2.9304	9.9397	16.9525
6	2.8216	9.4035	16.3217	2.9295	9.9230	16.9524
7	2.8165	9.3492	16.2094	2.9019	9.6689	16.7125
8	2.8163	9.3433	16.2061	2.9016	9.6467	16.6947
9	2.8163	9.3431	16.2061	2.8999	9.6458	16.6947
10	2.8163	9.3428	16.2060	2.8998	9.6455	16.6948

It is observed that increasing the number of polynomial items, n, improves the accuracy of results and leads to convergent solutions at $n = 10$. Hence $n = 10$ is used in the following numerical calculations.

4.1.2. Validation of the analysis

The validation analysis is done through direct comparison with previously published results and with finite element results obtained by using commercial finite element software package ANSYS [25].

4.1.2.1. Comparison with available results

In order to check the above written formulation, the first three frequency parameters of simply supported FG beams are compared with [26] for slenderness ratios ($L/h = 20$, 50 and 100) and power-law index ($k = 0$, 0.1 and 0.2). The material properties of steel are $E = 210$ GPa; $\rho = 2700$ Kg/m³ and those of Alumina (Al$_2$O$_3$) are $E = 390$ GPa; $\rho = 3960$ Kg/m³. Table 5 shows that the results given by the BT are very close to those available in [26].

Table 4. Convergence of first three frequency parameters of simply supported FG SWNT/Al-alloy beams using PSDBT for ($L/h = 5$) and 5 % SWNT content on the beam top surface

| PSDBT	Al-alloy			$k = 5$		
n	λ_1	λ_2	λ_3	λ_1	λ_2	λ_3
2	3.2955	13.5290	16.7497	3.3975	13.8882	17.09
3	2.8392	13.4896	16.5612	2.9222	13.8474	16.9789
4	2.8308	9.5187	16.4352	2.9136	9.7509	16.9519
5	2.8238	9.4449	16.3954	2.9059	9.6756	16.9328
6	2.8230	9.4275	16.3915	2.9051	9.6569	16.7576
7	2.8187	9.4247	16.3895	2.9011	9.6552	16.7579
8	2.8172	9.3961	16.3821	2.9008	9.6546	16.7575
9	2.8169	9.3957	16.3805	2.9005	9.6541	16.7574
10	2.8168	9.3955	16.3802	2.9005	9.6539	16.7574

Table 5. First three frequency parameters. A comparison with data after Amal et al. [26]

$L/h - k$		$L/h - k$		$L/h - k$		$L/h - k$	
20-0		50-0		100-0.1		100-0.2	
CBT	Ref	CBT	Ref	PSDBT	Ref	TBT	Ref
4.4019	4.3425	4.4038	4.3444	4.2526	4.2838	4.1372	4.2336
8.7903	8.6716	8.8054	8.6866	8.5009	8.5671	8.265	8.4666
13.152	12.975	13.2027	13.025	12.748	12.849	12.3952	12.699

4.1.2.2. Comparison with finite element resulats

As already mentioned, the material properties of the FG beam vary continuously throughout its thickness. The beam bottom surface is made of Al-alloy, whereas the top one is made of SWNT/Al-alloy composite. In order to model the FG beam, the numerical model has been divided into several layers so that the changes in properties can be made. Each layer has the finite portion of the thickness and treated like isotropic material. Material properties of each layer have been calculated at its mid-plane by using the chosen power-law distribution. To study the convergence analysis, various number of layers has been taken; 2, 4, 8 and 10. The FE modeling has been performed using ANSYS (2013). Higher order 3-D, 10-node elements (SOLID187) has been used for modeling of FG beams. SOLID187 has a quadratic displacement behavior. This element has three degrees of freedom at each node: translations in the nodal x, y, and z directions. To simulate the pin support, the x, y and z bottom edge displacements are constrained while the roller support is free to move in the axial direction. 208797 elements with 292166 nodes are needed. Fig. 5 shows the fundamental mode shape for 10 layers of simply supported FG SWNT reinforced Al-alloy composite beam. The materials used for modeling and analysis of beams are Al-alloy and Al-alloy comprising 10 % of SWNT. Their properties are given in the second and sixth lines of Table 1.
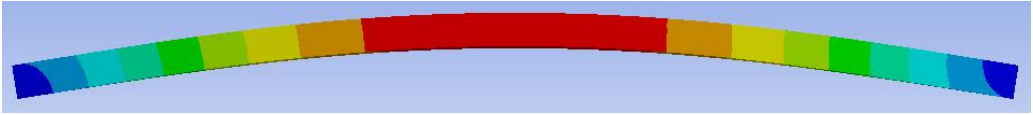
Fig. 5. Fundamental mode shape for 10 layers of FG beam

Table 6 reports the fundamental frequency parameters delivered by the FE analysis. Table 7 exposes the comparison between FE results and those obtained using the formulation explained in Section 3.

Interpretation: It can be interpreted that for different power-law distributions, the number of layers has a great influence on the fundamental frequencies of the modeled FG beam. From Table 6, one can consider that the convergence is reached for 10 layers. The FE results gotten for ten layers beams are confronted against those obtained using CBT, TBT and PSDBT. It is found that the present results are very close (see Table 7). The satisfactory results concerning the frequency parameters give confidence in the predictions reported in next sections.

Table 6. FE predictions of fundamental frequency parameters of simply supported FG SWNT/Al-alloy beams with ($L/h = 30$) and different power-law exponents (k)

N	$k = 0$	$k = 0.4$	$k = 1$	$k = 2$	$k = 5$	$k = 10$	Al-alloy
2	3.4668	3.3045	3.1576	3.0405	2.9247	2.8680	2.8500
4	3.4668	3.2825	3.1509	3.0686	2.9839	2.9184	2.8500
8	3.4668	3.2727	3.1496	3.0781	3.0057	2.9499	2.8500
10	3.4668	3.2718	3.1496	3.0795	3.0084	2.9546	2.8500

Table 7. Comparison of fundamental frequency parameters of simply supported FG SWNT/Al-alloy beams with FE results for different power-law exponents and slenderness ratio $L/h = 30$

Theory	$k = 0$	$k = 0.4$	$k = 1$	$k = 2$	$k = 5$	$k = 10$	Al-alloy
CBT	3.6698	3.4645	3.3477	3.2764	3.1982	3.1406	3.0168
TBT	3.6642	3.4593	3.3426	3.2713	3.1931	3.1355	2.9726
PSDBT	3.6642	3.4593	3.3426	3.2713	3.1930	3.1355	2.9726
FE	3.4668	3.2718	3.1496	3.0795	3.0084	2.9546	2.8500

4.2. Parametric study

A parametric study is carried out with CBT, TBT and PSDBT theories in order to predict the frequency parameters of simply supported FG SWNT reinforced Al-alloy composite beams. In this parametric investigation, various values of SWNT volume fractions, power-law index and slenderness ratios of the beams are taken into consideration.

Tables 8 and 9 show the fundamental frequency parameters of FG SWNT/Al-alloy composite beams for slenderness ratios $L/h = 5$ and 30, respectively and for different power-law exponents (k). The SWNT volume fraction incorporated in Al-alloy varies from 0 % on the bottom to 5 % on the beam top surface.

Tables 10 and 11 show the fundamental frequencies of FG SWNT/Al-alloy composite beams for slenderness ratios $L/h = 5$ and 30, respectively and for different power-law exponents (k). The SWNT volume fraction incorporated in Al-alloy varies from 0 % on the bottom to 10 % on the beam top surface.

Table 8. Fundamental frequency parameters of simply supported FG SWNT/Al-alloy beams with ($L/h = 5$) for 5 % SWNT content on the beam top surface

Theory	$k = 0$	$k = 0.4$	$k = 1$	$k = 2$	$k = 5$	$k = 10$	Al-alloy
CBT	3.3007	3.1954	3.1366	3.1009	3.0612	3.0319	2.9697
TBT	3.1305	3.0317	2.9748	2.9390	2.8998	2.8725	2.8163
PSDBT	3.1327	3.0344	2.9771	2.9403	2.9005	2.8736	2.8168

Table 9. Fundamental frequency parameters of simply supported FG SWNT/Al-alloy beams with ($L/h = 30$) for 5 % SWNT content on the beam top surface

Theory	$k = 0$	$k = 0.4$	$k = 1$	$k = 2$	$k = 5$	$k = 10$	Al-alloy
CBT	3.353	3.2461	3.1864	3.1499	3.1096	3.0798	3.0168
TBT	3.3478	3.2412	3.1814	3.1450	3.1046	3.0121	2.9726
PSDBT	3.3478	3.2412	3.1814	3.1449	3.1046	3.0121	2.9726

From Tables 8-11, it may be noted that for different power-law exponents and various SWNT contents, the three BT predict almost the same fundamental frequency parameters for $L/h = 30$ but for $L/h = 5$, predictions given by CBT are comparatively greater than that given by both TBT and PSDBT. As can be expected, for thick beams, effect of shear deformation becomes more significant and affects the results greatly. Thus, TBT and PSDBT are more efficient for thicker beams.

Table 10. Fundamental frequency parameters of simply supported FG SWNT/Al-alloy beams with ($L/h = 5$) for 10 % SWNT content on the beam top surface

Theory	$k = 0$	$k = 0.4$	$k = 1$	$k = 2$	$k = 5$	$k = 10$	Al-alloy
CBT	3.6125	3.4103	3.2955	3.2254	3.1486	3.0918	2.9697
TBT	3.4262	3.2366	3.1255	3.0555	2.9795	2.9263	2.8136
PSDBT	3.4289	3.2398	3.1279	3.0560	2.9784	2.9263	2.8168

Table 11. Fundamental frequency parameters of simply supported FG SWNT/Al-alloy beams with ($L/h = 30$) for 10 % SWNT content on the beam top surface

Theory	$k = 0$	$k = 0.4$	$k = 1$	$k = 2$	$k = 5$	$k = 10$	Al-alloy
CBT	3.6698	3.4645	3.3477	3.2764	3.1982	3.1406	3.0168
TBT	3.6642	3.4593	3.3426	3.2713	3.1931	3.1355	2.9726
PSDBT	3.6642	3.4593	3.3426	3.2713	3.1930	3.1355	2.9726

It is seen that for different SWNT volume fractions, the fundamental frequency parameter is decreasing with increasing k. It is illustrated that the variation in the low values of power exponent is more effective on the fundamental frequency parameter than the variation in high values of power exponent. The change in frequency parameter with respect to slenderness ratio is detrimental. The variation in fundamental frequency parameter is relatively high for higher slenderness ratio.

It can be observed that for a constant power exponent and a constant slenderness ratio, an increase in SWNT content on the beam top surface causes the increase in fundamental frequencies. This augmentation becomes more important for high slenderness ratio.

It is clearly shown that reinforcing Al-alloy with randomly oriented SWNT does not only improve the material properties of Al-alloy but also increase the fundamental frequency parameters. For 0.4 power-law exponent, compared to simply supported Al-alloy beam, the continuous variation of SWNT volume fraction to reach 5 % on the beam top surface increases the fundamental frequency parameter to 7.2. This improvement increases with both SWNT volume fraction and slenderness ratio.

Tables 12 and 13 present the first three frequency parameters of FG SWNT/Al-alloy composite beams for slenderness ratios $L/h = 5$ and 30, respectively and for different power-law exponents. The SWNT volume fraction incorporated in Al-alloy varies from 0 % on the bottom to 5 % on the beam top surface.

Tables 14 and 15 present the first three frequency parameters of FG SWNT/Al-alloy composite beams for slenderness ratios $L/h = 5$ and 30, respectively and for different power-law exponents. The SWNT volume fraction incorporated in Al-alloy varies from 0 % on the bottom to 10 % on the beam top surface.

Tables 16 and 17 summarize the first three frequency parameters of FG SWNT/Al-alloy composite beams considering 0.4 power-law exponent and two slenderness ratios $L/h = 5$ and 30. For the

top surface, 5 % and 10 % SWNT volume fractions are taken into account.

Table 12. First three frequency parameters of simply supported FG SWNT/Al-alloy beams with ($L/h = 5$) for 5 % SWNT content on the beam top surface

Theory	λ	$k = 0$	$k = 0.4$	$k = 1$	$k = 2$	$k = 5$	$k = 10$	Al-alloy
CBT	λ_1	3.3007	3.1954	3.1366	3.1009	3.0612	3.0319	2.9697
	λ_2	12.614	12.1989	11.9612	11.824	11.6857	11.582	11.3491
	λ_3	18.4948	17.9791	17.5889	17.2794	16.9618	16.8153	16.6401
TBT	λ_1	3.1305	3.0317	2.9748	2.939	2.8998	2.8725	2.8163
	λ_2	10.4479	10.1178	9.9131	9.7804	9.6455	9.5613	9.3428
	λ_3	18.2282	17.5708	17.202	16.9484	16.6948	16.5544	16.2060
PSDBT	λ_1	3.1327	3.0344	2.9771	2.9403	2.9005	2.8736	2.8168
	λ_2	10.444	10.1489	9.3009	9.7963	9.6539	9.5747	9.3955
	λ_3	18.2597	17.7054	17.3196	17.0344	16.7574	16.6318	16.3802

Table 13. First three frequency parameters of simply supported FG SWNT/Al-alloy beams with ($L/h = 30$) for 5 % SWNT content on the beam top surface

Theory	λ	$k = 0$	$k = 0.4$	$k = 1$	$k = 2$	$k = 5$	$k = 10$	Al-alloy
CBT	λ_1	3.353	3.2461	3.1864	3.1499	3.1096	3.0798	3.0168
	λ_2	13.3939	12.9596	12.713	12.567	12.4132	12.2991	12.0507
	λ_3	30.0753	29.1018	28.5499	28.2223	27.8752	27.6179	27.0593
TBT	λ_1	3.3478	3.2412	3.1814	3.145	3.1046	3.0121	2.9726
	λ_2	13.312	12.8811	12.6355	12.4894	12.3357	12.2224	11.8202
	λ_3	29.6658	28.7089	28.1621	27.8343	27.4875	27.2344	26.3414
PSDBT	λ_1	3.3478	3.2412	3.1814	3.1449	3.1046	3.0121	2.9726
	λ_2	13.312	12.8814	12.6356	12.489	12.3348	11.9771	11.8202
	λ_3	29.666	28.7103	28.1622	27.8321	27.4835	26.6912	26.3414

Table 14. First three frequency parameters of simply supported FG SWNT/Al-alloy beams with ($L/h = 5$) for 10 % SWNT content on the beam top surface

Theory	λ	$k = 0$	$k = 0.4$	$k = 1$	$k = 2$	$k = 5$	$k = 10$	Al-alloy
CBT	λ_1	3.6125	3.4103	3.2955	3.2254	3.1486	3.0918	2.9697
	λ_2	13.8058	12.9904	12.505	12.231	11.9811	11.7951	11.3491
	λ_3	20.2422	19.2589	18.5128	17.9138	17.2861	16.9914	16.6401
TBT	λ_1	3.4262	3.2366	3.1255	3.0555	2.9795	2.9263	2.8136
	λ_2	11.435	10.7922	10.3847	10.1237	9.8692	9.7117	9.3428
	λ_3	19.8507	18.7512	18.0276	17.5329	17.0461	16.7779	16.206
PSDBT	λ_1	3.4289	3.2398	3.1279	3.056	2.9784	2.9263	2.8168
	λ_2	11.4648	10.8288	10.4117	10.1311	9.8605	9.713	9.3955
	λ_3	19.9862	18.9062	18.1507	17.5943	17.0578	19.8185	16.3802

Table 15. First three frequency parameters of simply supported FG SWNT/Al-alloy beams with ($L/h = 30$) for 10 % SWNT content on the beam top surface

Theory	λ	$k = 0$	$k = 0.4$	$k = 1$	$k = 2$	$k = 5$	$k = 10$	Al-alloy
CBT	λ_1	3.6698	3.4645	3.3477	3.2764	3.1982	3.1406	3.0168
	λ_2	14.6593	13.8149	13.3206	13.0321	12.7448	12.5322	12.0507
	λ_3	32.9168	31.0264	29.9232	29.2765	28.6256	28.1438	27.0593
TBT	λ_1	3.6642	3.4593	3.3426	3.2713	3.1931	3.1355	2.9726
	λ_2	14.5697	13.6704	13.24	12.9515	12.664	12.4527	11.8202
	λ_3	32.4687	30.6109	29.5193	28.8724	28.2207	27.7461	26.3414
PSDBT	λ_1	3.6642	3.4593	3.3426	3.2713	3.193	3.1355	2.9726
	λ_2	14.5698	13.7324	13.2401	12.9505	12.6621	12.4515	11.8202
	λ_3	32.469	30.6134	29.5196	28.8679	28.2121	27.7401	26.3414

Table 16. First three frequency parameters of simply supported FG SWNT/Al-alloy beams with $k = 0.4$ for 5 % SWNT content on the beam top surface

Theory	L/h	λ_1	λ_2	λ_3
CBT	5	3.4103	12.9904	19.2589
	30	3.4645	13.8149	31.0264
TBT	5	3.2366	10.7922	18.7512
	30	3.4593	13.6704	30.6109
PSDBT	5	3.2398	10.8288	18.9062
	30	3.4593	13.7324	30.6134

Table 17. First three frequency parameters of simply supported FG SWNT/Al-alloy beams with $k = 0.4$ for 10 % SWNT content on the beam top surface

Theory	L/h	λ_1	λ_2	λ_3
CBT	5	3.1096	12.4132	27.8752
	30	3.1096	12.4132	27.8752
TBT	5	2.8998	9.6455	16.6948
	30	3.1046	12.3357	27.4875
PSDBT	5	2.9005	9.6539	16.7574
	30	3.1046	12.3348	27.4835

Same remarks and conclusions, deduced from Tables 8-11, concerning the effect of different variables (SWNT distribution, SWNT volume fraction and slenderness ratio) on the fundamental frequency parameters can be noted from Tables 12-17 for the three first frequency parameters. The frequency parameters are increasing with increase in slenderness ratios (L/h) and are decreasing with increase in power-law exponents (k). It is also seen that for $L/h = 5$, the results for FG beam using CBT are comparatively greater than those found using other BT, where as for $L/h = 30$, one may experience mere coincidence of frequency parameters. This due to the deficiency in Euler beam theory for consideration the shear effect, which affects significant on the frequencies especially for the short beam. Moreover, it is very important to see that the variable parameters have more influence on the second and third frequency parameters than that on the fundamental frequency parameter. For 0.4 power-law exponent, compared to simply supported Al-alloy beam, the continuous variation of the SWNT volume fraction to reach 10 % on the beam top surface increases the frequency parameters to at least 13.5. This improvement increases with both the SWNT volume fraction and the slenderness ratio.

5. Conclusions

The free vibration of simply supported FG SWNT/Al-alloy beam was investigated based on various BT using the Rayleigh-Ritz method. This helps fill in a gap in the literature where the available mechanical results about SWNT reinforced Al-alloy composites did not concern the free vibration. The Rayleigh-Ritz method is found to be efficient when compared to FE simulations. The objective of improving the dynamic characteristics of Al-alloy in order to prevent problems such as failures associated with resonance and fatigue is achieved by reinforcing with functionally graded SWNT. Reinforcement with SWNT allows a significant increase of the Al-alloy dynamic properties without compromising other factors such as mass of the structure. The improvement of the natural frequencies of beams made of AL-alloy was attained by increasing the amount of the reinforcement, increasing the slenderness ratio and decreasing the power-law exponent.

References

[1] **Shen H. S.** Nonlinear bending of functionally graded carbon nanotube reinforced composite plates in thermal environment. Composite Structures, Vol. 91, 2009, p. 9-19.

[2]   **Rashidifar M. A., Ahmadi D.** Vibration analysis of randomly oriented carbon nanotube based on FGM beam using Timoshenko theory. Advances in Mechanical Engineering, 2014, https://doi.org/10.1155/2014/653950.

[3]   **Chowdhury S. C., Okabe T.** Computer simulation of carbon nanotube pull-out from polymer by the molecular dynamics method. Composites Part A, Vol. 38, 2007, p. 747-754.

[4]   **Udupa G., Rao S. S., Gangadharan K. V.** Fabrication of functionally graded carbon nanotube-reinforced aluminum matrix laminate by mechanical powder metallurgy technique – part I. Material Science and Engineering, Vol. 4, Issue 3, 2015, p. 1000169.

[5]   **Mansoor M., Shahid M.** Carbon nanotube-reinforced aluminum composite produced by induction melting. Journal of Applied Research and Technology, Vol. 14, 2016, p. 215-224.

[6]   **Richter V.** Fabrication and properties of gradient hard metals. Proceedings of the 3rd International Symposium on Structural and Functional Gradient Materials, 1994, p. 587-592.

[7]   **Selmi A., Friebel C., Doghri I., Hassis H.** Prediction of the elastic properties of single walled carbon nanotube reinforced polymers: a comparative study of several micromechanical models. Composites Science and Technology, Vol. 67, 2007, p. 2071-2084.

[8]   **Odegard G. M., Gates T. S., Wise K. E., Park C., Siochi E. J.** Constitutive modelling of nanotube reinforced polymer composites. Composites Science and Technology, Vol. 63, 2003, p. 1671-1687.

[9]   **Heshmati M., Yas M. H.** Free vibration analysis of functionally graded CNT-reinforced nanocomposite beam using Eshelby-Mori-Tanaka approach. Journal of Mechanical Science and Technology, Vol. 27, 2013, p. 3403-3408.

[10]   **Shenas A. G., Malekzadeh P., Ziaee S.** Vibration analysis of pre-twisted functionally graded carbon nanotube reinforced composite beams in thermal environment. Composite Structures, Vol. 162, 2017, p. 325-340.

[11]   **Yas M. H., Samadi N.** Free vibrations and buckling analysis of carbon nanotube-reinforced composite Timoshenko beams on elastic foundation. International Journal of Pressure Vessels and Piping, Vol. 98, 2012, p. 119-128.

[12]   **Ke L. L., Yang J., Kitipornchai S.** Nonlinear free vibration of functionally graded carbon nanotube-reinforced composite beams. Composite Structures, Vol. 92, 2010, p. 676-83.

[13]   **Wu H. L., Yang J., Kitipornchai S.** Nonlinear vibration of functionally graded carbon nanotube-reinforced composite beams with geometric imperfections. Composites Part B, Vol. 90, 2016, p. 86-96.

[14]   **Ansari R., Faghih Shojaei M., Mohammadi V., Gholami R., Sadeghi F.** Nonlinear forced vibration analysis of functionally graded carbon nanotube-reinforced composite Timoshenko beams. Composite Structures, Vol. 113, 2014, p. 316-327.

[15]   **Nejati M., Eslampanah A., Najafizadeh M. H.** Buckling and vibration analysis of functionally graded carbon nanotube-reinforced beam under axial load. International Applied Mechanics, Vol. 8, 2016, p. 1650008.

[16]   **Yas M. H., Heshmati M.** Dynamic analysis of FG nano-composite beam reinforced by randomly oriented carbon nanotube under the action of moving load. Applied Mathematical Modelling, Vol. 36, 2012, p. 1371-1394.

[17]   **Roufaeil O. L., Dawe D. J.** Rayleigh-Ritz vibration analysis of rectangular Mindlin plates subjected to membrane stresses. Journal of Sound and Vibration, Vol. 85, 1980, p. 263-275.

[18]   **Chakraverty S.** Vibration of Plates. CRC Press, Taylor and Francis Group, 2009.

[19]   **Zainuddin H. B., Ali M. B.** Study of wheel rim impact test using finite element analysis. Proceedings of Mechanical Engineering Research Day, 2016.

[20]   **Eatemadi A., Daraee H., Karimkhanloo H., Kouhi M., Zarghami N., Akbarzadeh A., Abasi M., Hanifehpour Y., Joo S. W.** Carbon nanotubes: properties, synthesis, purification, and medical applications. Nanoscale Research Letters, Vol. 9, 2014, p. 393.

[21]   **Friebel C., Doghri I., Legat V.** General mean-field homogenization schemes for viscoelastic composites containing multiple phases of coated inclusions. International Journal of Solids and Structures, Vol. 43, Issue 9, 2006, p. 2513-2541.

[22]   **Aydogdu M., Taskin V.** Free vibration analysis of functionally graded beams with simply-supported edges. Materials and Design, Vol. 28, 2007, p. 1651-1656.

[23]   **Simsek M.** Fundamental frequency analysis of functionally graded beams by using different higher-order beam theories. Nuclear Engineering and Design, Vol. 240, 2010, p. 697-705.

[24]   **Pradhan K. K., Chakraverty S.** Effects of different shear deformation theories on free vibration of functionally graded beams. International Journal of Mechanical Sciences, Vol. 82, 2014, p. 149-160.

[25] ANSYS workbench 13.0.1. ANSYS, 2013.

[26] **Amal E. A., Eltaher M. A., Mahmoud F. F.** Free vibration characteristics of a functionally graded beam by finite element method. Applied Mathematical Modelling, Vol. 35, 2011, p. 412-425.

Abdellatif Selmi received his Ph.D. degree in civil engineering from Tunis El Manar University, Tunis, Tunisia, in 2008. Now he works at Prince Sattam bin Abdulaziz University. His current research interests include composite material and mechanical vibration.

Awni Bisharat received his Ph.D. degree in mechanical engineering from All-Russian Research Institute of Meat Industry, Moscow, Russia, in 1997. Now he works at Prince Sattam Bin Abdulaziz University. His current research interests include manufacturing processes and mechanical vibration.